

9:30am - 9:45am
FC4

Zero-Dispersion Wavelength Distribution in Optical Fibers from CW Four-Wave Mixing

John B. Schlager

National Institute of Standards and Technology, 325 Broadway, Boulder, CO 80303

Maximum four-wave mixing (FWM) efficiency in an optical fiber occurs at or near the fiber's zero-dispersion wavelength λ_0 .¹ In fiber samples with uniform chromatic dispersion, a good estimate of λ_0 can be made by determining the wavelength of maximum FWM efficiency in an end-to-end fiber measurement using unmodulated (cw) laser sources.² However, if λ_0 varies appreciably (by > 0.5 nm) along the length of the fiber, a simple end-to-end measurement of maximum FWM efficiency will give only a rough approximation of the path-averaged λ_0 and little information on how λ_0 varies with length.² To address this problem, others have used pulsed laser sources and/or optical time-domain reflectometry with FWM or other nonlinear effects to map the zero-dispersion wavelength distribution.³⁻⁵ These techniques are complex and can require special high-power laser sources. More recently, Brener, et al. used cw FWM with a phase retrieval algorithm to estimate the length distribution of λ_0 .⁶ This letter describes a similar FWM efficiency measurement technique that uses low-power cw laser sources to obtain end-to-end FWM efficiency curves for forward- and backward-propagating light and then uses these data to estimate the length distribution of λ_0 with a numerical algorithm that models FWM efficiency in fiber. Unlike the technique used by Brener, only one laser source is actively tuned during the measurement scan. The second source remains fixed in wavelength.

The experimental configuration for obtaining FWM efficiency has been described previously.² Two tunable lasers provide the pump and probe lights. The pump laser is amplified with an erbium-doped fiber amplifier (EDFA) to a power of 10 mW. The probe laser light at 0.5 mW is mechanically chopped to allow narrow-band detection of the FWM signal with lock-in amplifier techniques. Light from each source passes through a tunable optical bandpass filter to minimize the amplified spontaneous emission light, which can overwhelm the FWM signal, and polarization controllers are used to bring the polarization states into coincidence. The pump

and probe lights are combined in a fused-fiber coupler, traverse the test fiber, and continue on to the photoreceiver. An additional tunable bandpass filter is used at the photoreceiver to further isolate the FWM signal. The detected signal is passed to a lock-in amplifier. A computer automatically tunes the pump laser and bandpass filters, and acquires the FWM efficiency data. Path-averaged and cutback measurements of λ_0 are made with a frequency-domain phase shift (FDPS) system used at NIST for fiber calibration standards.⁷ Laser wavelengths are measured with an interferometric wavemeter having an accuracy of 1 ppm.

The path-averaged, zero-dispersion wavelength for a ~ 10 km spool of dispersion-shifted fiber is first measured using the FDPS system. Next, the test fiber is placed in the FWM system, and a FWM efficiency curve is generated by monitoring the FWM light while the pump is scanned through the fiber's path-averaged λ_0 . The probe wavelength remains fixed at a mean pump-probe separation of approximately 10 nm. The measurement is repeated with the fiber ends reversed to obtain a FWM efficiency curve for light propagating in the opposite direction. These efficiency curves will differ from each other if λ_0 varies with length and the fiber has loss. The path-averaged λ_0 , the dispersion slope at λ_0 , the fiber loss, and the two FWM efficiency curves serve as inputs to the computer algorithm. The algorithm treats the fiber as if it were composed of multiple sections, each having a constant λ_0 . It solves the wave equation describing FWM for each section subject to the boundary conditions at the section ends.¹ The algorithm calculates the expected end-to-end FWM efficiency curves for numerous λ_0 profiles while keeping track of how these curves differ from the curves obtained empirically. Candidate profiles are chosen with sufficiently smooth character to be physically reasonable for a continuous sample of fiber that contains no splices. Profiles that generate FWM efficiency curves that differ little from the empirical

forward and backward efficiency curves while maintaining a path-averaged λ_0 consistent with the FDPS result are assumed to approximate the actual λ_0 profile of the fiber. A good match between measured and calculated efficiency curves is determined by minimizing the sum of the squared deviations between the calculated and measured FWM efficiency curves.

FWM efficiency measurements were made on two ~ 10 km fiber samples. Measured and calculated FWM efficiency curves for forward propagation in both fibers are shown in Fig. 1. To obtain the calculated curves, the first fiber

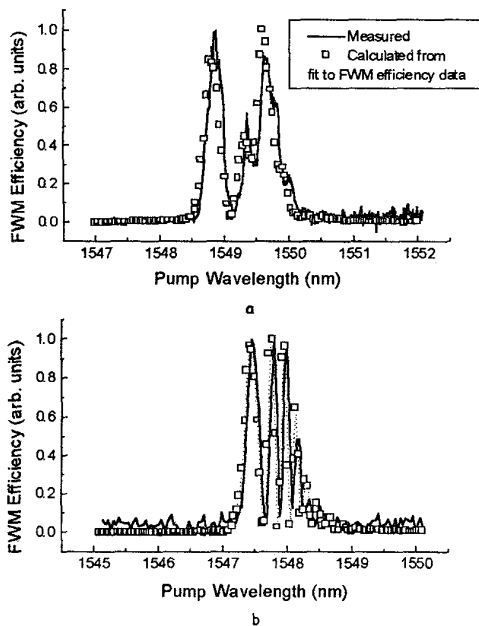


Fig. 1 Measured and calculated FWM efficiency curves for forward propagation in two 10 km samples- (a) first fiber, (b) second fiber

was modeled as 100 sections of constant λ_0 ; the second fiber was modeled as 40 sections of constant λ_0 . The associated length distributions of λ_0 determined from both the calculation and from cutback measurements using the FDPS system are shown in Figs. 2 and 3. Cutback measurements were made on four 2.5 km sections in the first fiber and ten 1 km sections in the second fiber. Measured path-averaged values for the first fiber are within 0.09 nm of the associated path-averaged values determined by the calculation. This discrepancy is no larger than 0.16 nm for the second fiber.

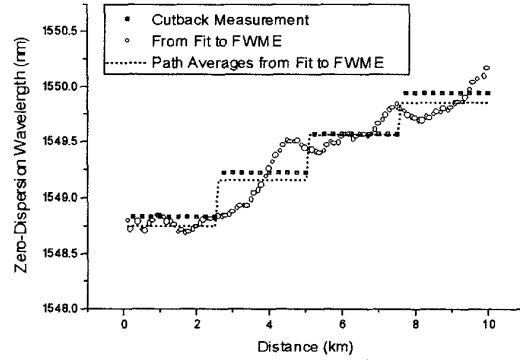


Fig. 2 Length Distribution of λ_0 for the first 10 km fiber determined from calculation and from cutback measurements using the freq.-domain phase shift system

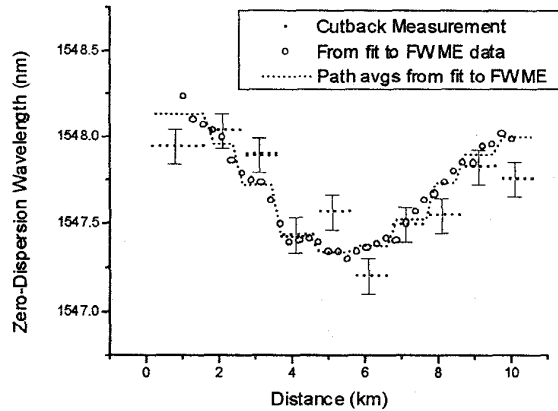


Fig. 3 Length distribution of λ_0 for the second 10 km fiber determined from calculation and from cutback measurements using the freq.-domain phase shift system

REFERENCES

- 1 Inoue, K., *J. Lightwave Technol.*, vol. 10, pp. 1553-1561, 1992.
- 2 Schlager, J.B., Mechels, S.E., and Franzen, D.L., *Proc. Symp. Optical Fiber Meas., SOFM'96*, Boulder, Colorado, 1996, pp. 121-124.
- 3 Nishi, S. and Saruwatari, M., *Electron. Lett.*, vol. 31, pp. 225-226, 1995.
- 4 Jopson, R.M., Eiselt, M., Stolen, R.H., Derosier, R.M., Vengsarkar, A.M., and Koren, U., *Electron. Lett.*, vol. 31, pp. 2115-2117, 1995.
- 5 Mollnauer, L.F., Mamyshev, P.V. and Neubelt, M.J., *Opt. Lett.*, vol. 21, pp. 1724-1726, 1996.
- 6 Brener, I., Mitra, P.P., and Thomson, D.J., in *Tech. Digest Optical Fiber Communications Conference, OFC'98*, San Jose, California, 1998, paper ThR5, pp. 344-345.
- 7 Mechels, S.E., Schlager, J.B., and Franzen, D.L., *J. Res. Natl. Inst. Stand Technol.*, vol. 102, pp. 333-347, 1997.